

UV Raman spectroscopic studies of V/ θ -Al₂O₃ catalysts in butane dehydrogenation

Zili Wu^a, Peter C. Stair^{a,b,*}

^a Department of Chemistry, Center for Catalysis and Surface Science and Institute of Environmental Catalysis, Northwestern University, Evanston, IL 60208, USA

^b Chemistry Division, Argonne National Laboratory, Argonne, IL 60439, USA

Received 25 August 2005; revised 1 November 2005; accepted 3 November 2005

Available online 6 December 2005

Abstract

To explore the coke formation mechanism and catalyst structure under alkane dehydrogenation (DH) conditions, the DH of butane on V/ θ -Al₂O₃ was explored by in situ UV Raman spectroscopy and reactivity tests. Studies of butane DH on V/ θ -Al₂O₃ catalysts with various distributions of surface VO_x species identify a structure–coke relationship. The deactivation of the catalysts in butane DH is due mainly to the formation of coke species. Both the nature and amount of coke formed are related to the structure of VO_x species. Monovanadates make chain-like polyaromatics, whereas polyvanadates produce mainly sheet-like (two-dimensional) polyaromatics that are detrimental to catalytic activity. The amount of coke formed from butane DH follows this sequence: polymeric VO_x > monomeric VO_x > V₂O₅, Al₂O₃. Raman spectroscopy studies of butane, 1-butene, *cis/trans*-2-butenes, and 1,3-butadiene reactions on V/ θ -Al₂O₃ catalysts enable the formulation of a coke formation pathway for butane DH, in which polystyrene is found to be a key intermediate. Although the surface of V/ θ -Al₂O₃ is partially reduced under butane DH conditions, the structure of VO_x species can be fully regenerated by oxidation of the coke species at temperatures up to 873 K.
© 2005 Elsevier Inc. All rights reserved.

Keywords: Dehydrogenation; Butane; Vanadium oxide; Monovanadate; Polyvanadate; UV Raman; Coke; Polyaromatics; Polystyrene

1. Introduction

The increasing demand for light olefins and the insufficient capacity of current production by steam and catalytic cracking are the driving forces behind the investigation of alternative ways to manufacture these chemicals [1,2]. Currently, the most feasible processes on a commercial scale are catalytic dehydrogenation (DH) and oxidative dehydrogenation (ODH) of light alkanes [1,3–8]. Commercial catalysts for alkane DH processes are supported chromium oxide and platinum metal [9,10]. In both systems, the catalytic DH reaction is accompanied by various competing reactions, including significant carbon laydown, resulting in catalyst deactivation. The possibility of using oxide systems other than chromia is being explored in an effort to make the alkane–olefin conversion process more selective and stable. Supported vanadium oxide (VO_x) catalysts for the

ODH of light alkanes have been studied extensively [1,3–8]. They have also been explored in the DH of light alkanes, including propane and butane [11–15], and show promise to be both active and selective for DH reactions. For example, depending on the pretreatment methods, V/Al₂O₃ can catalyze the DH of butanes at 853 K with conversion up to about 50% and selectivity to 90% [13]. Meanwhile, deactivation of VO_x catalysts by coke species is also observed with time on stream in butane DH reactions. However, due to the limited number of studies on supported VO_x for alkane DH, many questions remain unanswered; for example, the structure of supported VO_x and the mechanism of deactivation/coke deposition under DH conditions are unclear.

The focus of this study is to investigate the structure of surface VO_x and the coke formation process during butane DH over V/ θ -Al₂O₃ catalysts with various surface VO_x densities (0.03–14.2 V/nm²) using in situ UV Raman spectroscopy. Our recent study [16] suggested the existence of three types of VO_x species—monovanadate, polyvanadate, and V₂O₅—on the surface of θ -Al₂O₃. The distribution of these VO_x species de-

* Corresponding author.

E-mail address: pstair@northwestern.edu (P.C. Stair).

depends on the surface VO_x density. Monovanadate is the only species on the sample with VO_x density $\leq 0.16 \text{ V/nm}^2$; polyvanadates coexist with monovanadate on samples with a surface VO_x density of 1.2 V/nm^2 , and a mixture of monovanadate, polyvanadates and crystalline V_2O_5 is found on samples with surface VO_x density $> 1.2 \text{ V/nm}^2$. Because these $\text{V}/\theta\text{-Al}_2\text{O}_3$ samples feature a wide distribution of different surface VO_x species, a study of butane DH catalyzed by them may identify a structure–reactivity correlation, specifically, a structure–coke formation relationship. We expect that a better understanding of coke formation chemistry and the role of different VO_x species in coke formation during butane DH can be reached, which will facilitate optimization of the catalysts and possible reduction of side reactions leading to coke.

2. Experimental

2.1. Catalyst preparation

All $\text{V}/\theta\text{-Al}_2\text{O}_3$ samples with surface VO_x density in the range $0.03\text{--}14.2 \text{ V/nm}^2$ were prepared via incipient wetness impregnation of $\theta\text{-Al}_2\text{O}_3$ (Johnson Matthey; $S_{\text{BET}} = 101 \text{ m}^2/\text{g}$) with aqueous NH_4VO_3 (99+%, Aldrich) solutions. Oxalic acid (99%, Aldrich) [$\text{NH}_4\text{VO}_3/\text{oxalic acid} = 0.5$ (molar ratio)] was added into the solutions for high VO_x loadings to ensure the dissolution of NH_4VO_3 . A $\text{V}/\theta\text{-Al}_2\text{O}_3$ sample with surface VO_x density of $Y \text{ V/nm}^2$ is denoted by YV in what follows. After impregnation, the samples were dried at room temperature by purging with air, heated at 393 K overnight, and finally calcined at 823 K for 6 h in air.

2.2. Raman studies

In situ UV (244 nm) Raman studies of butane DH on various $\text{V}/\theta\text{-Al}_2\text{O}_3$ catalysts were conducted on a Raman instrument built at Northwestern University [17,18]. Some of the Raman spectra were collected on a Triax 550 single-grating spectrograph with a UV-enhanced CCD detector. A UV edge filter (Barr Associates) was used to block Rayleigh scattering. The 244-nm excitation is produced by a Lexel 95 SHG (second harmonic generation) laser equipped with an intracavity nonlinear crystal, BBO (beta barium borate; BaB_2O_4), which frequency doubles visible radiation into the mid-ultraviolet region. Raman spectra were collected under a controlled atmosphere using a fluidized bed reactor described previously [19]. The laser power and spot size at the sample position were ca. 2 mW and $50 \mu\text{m}$, respectively. Data collection times varied from 60 s to 4 h , depending on the signal level. The Raman shift was calibrated by measuring several liquid standards, including cyclohexane, acetonitrile, acetone, chloroform, ethyl acetate, toluene, and benzene. A mathematical procedure involving a quadratic fit of the observed to the actual wavenumbers of the standards was used for the calibration. The band positions in the Raman spectra were determined using the program PeakFit v4.11.

In the Raman study of butane DH, the sample was first either calcined ($5\% \text{ O}_2/\text{N}_2$, 60 ml/min) at 823 K or reduced ($5\% \text{ H}_2/\text{N}_2$, 60 ml/min) at 873 K for 60 min in the fluidized-bed

reactor, and then purged with He (60 ml/min) for 10 min before being exposed to $3\% \text{ butane}/\text{N}_2$ (60 ml/min) at different temperatures ($373\text{--}873 \text{ K}$) for 30 min . The sample was then purged with He at reaction temperature for another 10 min , to remove any adsorbed hydrocarbon species before spectral measurements. Raman spectra were collected at both reaction temperature and room temperature in flowing He (150 ml/min). The spectra collected at reaction temperature are nearly identical to those collected at room temperature except for the difference in band intensities due to thermal effects [20]. All of the spectra shown here were collected at room temperature. Each experiment was conducted in a sequence of measurements after progressively higher temperature treatments. Raman studies of $3\% \text{ 1-butene}/\text{N}_2$, $3\% \text{ cis-2-butene}/\text{N}_2$, $3\% \text{ trans-2-butene}/\text{N}_2$, and $1.4\% \text{ 1,3-butadiene}/\text{N}_2$ on $\text{V}/\theta\text{-Al}_2\text{O}_3$ catalysts were conducted using the same procedure as for butane DH. After reaction at 873 K , the catalyst was usually oxidized in a $2\% \text{ O}_2/\text{N}_2$ flow (60 ml/min) in the fluidized bed reactor at different temperatures ($473\text{--}873 \text{ K}$) for 1 h . Raman spectra of the reoxidized catalyst were then collected at room temperature in flowing He.

2.3. Activity test and temperature-programmed oxidation (TPO)

Due to the large void volume of the fluidized-bed reactor used in the Raman studies, a U-shaped microreactor was used in tests of $\text{V}/\theta\text{-Al}_2\text{O}_3$ catalysts for butane DH activity. The sample (ca. 0.3 g) was heated to 873 K in $5\% \text{ O}_2/\text{N}_2$ (60 ml/min) and held at this temperature for 2 h . After calcination, the sample was purged with He to remove all oxygen in the system and then exposed to a $1.5\% \text{ butane}/\text{N}_2$ stream with a total flow rate of 120 ml/min . The reaction was usually run for 90 min . On-line gas analysis was performed using an Agilent 3000 Micro GC equipped with a Plot U, a Molsieve 5A, and an Alumna Plot column and TCD detectors. It takes about 10 min for the gas flow to be stabilized in the reaction system for GC analysis and each sampling runs for 160 s . Negligible conversion ($<2\%$) of butane was observed in the gas phase and on $\theta\text{-Al}_2\text{O}_3$ at 873 K .

After activity tests, the coked catalyst was purged with He at reaction temperature for another 10 min and then cooled to room temperature in He. Temperature-programmed oxidation (TPO) of the catalyst was then conducted in a $5\% \text{ O}_2/\text{N}_2$ (60 ml/min) flow with a heating rate of 5 K/min . O_2 , CO_2 , and CO components were monitored during the TPO process using the Agilent 3000 Micro gas chromatograph. The amount of coke is expressed as monolayers. Assuming that the coke is pure carbon (hydrogenated carbon will make little difference to the calculation), a monolayer of coke on the catalyst surface corresponds to $10^{19} \text{ C-atom/m}^2$ (this is the value for most solids) [21]. The monolayer of coke is calculated with respect to the available surface area of Al_2O_3 in each catalyst.

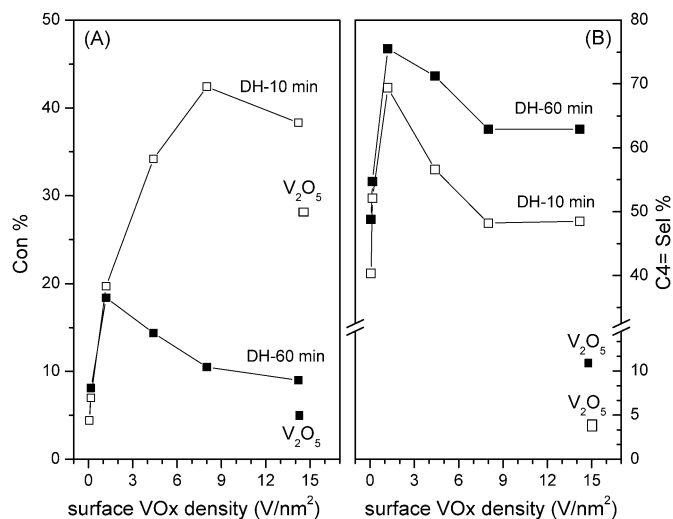


Fig. 1. (A) Conversion of butane DH at 873 K on $V/\theta\text{-Al}_2\text{O}_3$ catalysts at different reaction time as a function of surface VO_x density. (B) Selectivity of $\text{C}_4=$ in butane DH at 873 K on $V/\theta\text{-Al}_2\text{O}_3$ catalysts at different reaction time as a function of surface VO_x density.

3. Results

3.1. Catalytic performance of $V/\theta\text{-Al}_2\text{O}_3$ for butane DH

The $V/\theta\text{-Al}_2\text{O}_3$ catalysts with surface VO_x densities of 0.03–14.2 V/nm^2 were tested for butane DH at 873 K. The activity and selectivity data on different catalysts plus bulk V_2O_5 are compared in Fig. 1. The initial activity increases as a function of surface VO_x density up to 8 V/nm^2 and then declines on the 14.2V catalyst, and further declines on bulk V_2O_5 . With prolonged time on stream (i.e., DH for 60 min), butane conversion decreases dramatically on the catalysts with surface VO_x density $> 1.2 \text{ V}/\text{nm}^2$, whereas it remains nearly unchanged on those catalysts with surface VO_x density $\leq 1.2 \text{ V}/\text{nm}^2$. The decrease in activity is due mainly to the formation of coke deposits and blocking of surface sites throughout the reaction, as determined by Raman studies. The selectivity plot of C_4 olefins, including 1-butene, *cis*-2-butene, *trans*-2-butene, and 1,3-butadiene, features a volcano shape as a function of surface VO_x density, with a peak value observed on the 1.2V sample. Other reaction products from butane DH are $\text{C}_1\text{--C}_3$ hydrocarbons from cracking, CO_x , and carbon deposits on the catalyst surface. The C_4 olefins are distributed as follows: 1,3-butadiene $> 1\text{-butene} \approx \textit{trans}\text{-2-butene} > \textit{cis}\text{-2-butene}$. Using thermodynamic data from the literature [22,23], the thermodynamic conversion at 900 K is close to 100%, and the selectivity to C_4 olefins follows the sequence: 1,3-butadiene $> \textit{trans}\text{-2-butene} > \textit{cis}\text{-2-butene} \approx 1\text{-butene}$. The differences between the calculated and measured partial pressures indicate that the reaction has not reached thermodynamic equilibrium. The $\text{C}_4=$ selectivity increases on all catalysts as the reaction time increases from 10 to 60 min. A rather stable value of selectivity is actually obtained after 30 min. Among all VO_x catalysts, 1.2V gives the highest olefin selectivity, with a stable value of ca. 76%. Clearly, the 1.2V catalyst has the best performance among the

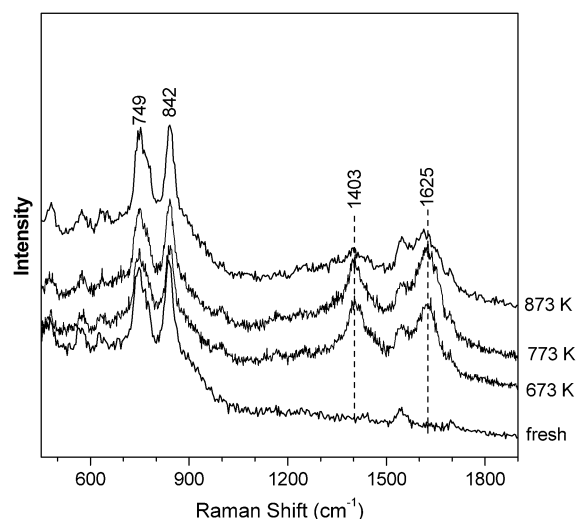


Fig. 2. Raman spectra of butane DH on $\theta\text{-Al}_2\text{O}_3$ at different temperatures.

$V/\theta\text{-Al}_2\text{O}_3$ catalysts studied for butane DH in terms of activity, stability, and selectivity.

3.2. Raman study of butane DH

3.2.1. Butane DH on $\theta\text{-Al}_2\text{O}_3$

Fig. 2 shows the Raman spectra after butane DH on pure $\theta\text{-Al}_2\text{O}_3$ at different temperatures. The Raman bands below 900 cm^{-1} are due to $\theta\text{-Al}_2\text{O}_3$, and their intensity remains essentially unchanged on butane DH at increasing temperatures. New bands at 1625 and 1403 cm^{-1} observed at reaction temperatures of 673–873 K are due to hydrocarbon deposits formed from the reaction. The two bands can be assigned to the $\text{C}=\text{C}$ stretch and $\text{C}\text{--H}$ deformation, respectively, characteristic of olefin/polyolefin species [18,24–26]. Considering the relative intensity of the bands due to coke species compared with those of the $\theta\text{-Al}_2\text{O}_3$ support, the amount of coke deposited is quite small, as was confirmed in the TPO studies.

3.2.2. Butane DH on $V/\theta\text{-Al}_2\text{O}_3$ Catalysts

Raman studies of butane DH were conducted on $V/\theta\text{-Al}_2\text{O}_3$ catalysts with surface VO_x density of 0.03–14.2 V/nm^2 . Raman spectra from three representative $V/\theta\text{-Al}_2\text{O}_3$ samples with different distributions of surface VO_x species were selected for discussion here: the 0.03V sample with only monovanadate on the surface, the 1.2V sample with monovanadate and polyvanadates, and the 14.2V sample with a mixture of monovanadate, polyvanadates, and crystalline V_2O_5 .

Fig. 3A shows the Raman spectra of the oxidized 0.03V sample after butane DH at different temperatures. The bands at 910 and 1014 cm^{-1} on the oxidized sample are due to surface VO_x species and are assigned to $\text{V}\text{--O}\text{--Al}$ and $\text{V}=\text{O}$ vibrations, respectively [16]. The bands due to VO_x species and $\theta\text{-Al}_2\text{O}_3$ show intensity changes only at a reaction temperature of 873 K. The decrease in intensity of bands due to VO_x species at 873 K is likely due to a combination of VO_x reduction [5,27–30] and optical absorption by coke species. The Raman bands due to coke species observed below 873 K at 1613 and 1410 cm^{-1} are

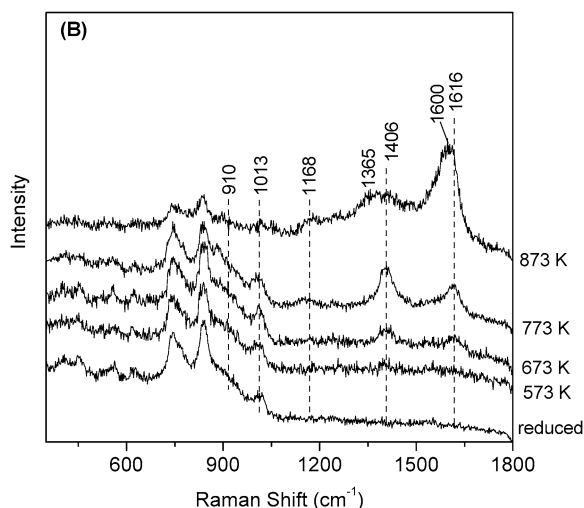
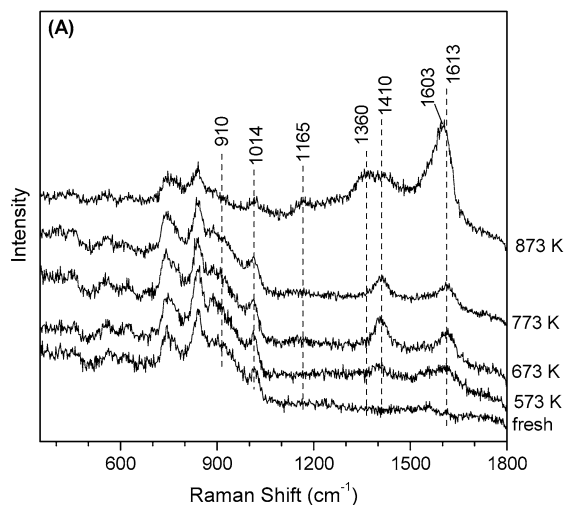


Fig. 3. Raman spectra of butane DH on (A) oxidized and (B) pre-reduced 0.03V at different temperatures.

due to polyolefins/polyaromatics. At a reaction temperature of 873 K, new bands due to coke species develop: a weak band at 1165 cm^{-1} , a broad feature at 1360 cm^{-1} , and an intense one at 1603 cm^{-1} . The band at 1165 cm^{-1} is attributable to C–H bending, and the other two are due to ring stretching in polyaromatic compounds [24–32]. Fig. 3B presents the Raman spectra from butane DH on a reduced 0.03V sample at different temperatures. The 873 K-reduced 0.03V sample gives a Raman band due to the V=O stretch at 1013 cm^{-1} , whereas the band due to V–O–Al observed on an oxidized sample is hardly detectable. The decrease in relative intensity of the bands due to VO_x species compared with $\theta\text{-Al}_2\text{O}_3$ suggests that the surface VO_x species are partially reduced in H_2 at 873 K. When subjected to butane DH at high temperatures, the pre-reduced sample produces similar Raman bands due to coke species as those on its oxidized counterpart (cf. Figs. 3A and B). It seems that the initial oxidation state of surface VO_x species does not affect the nature of coke species formed in butane DH. This re-

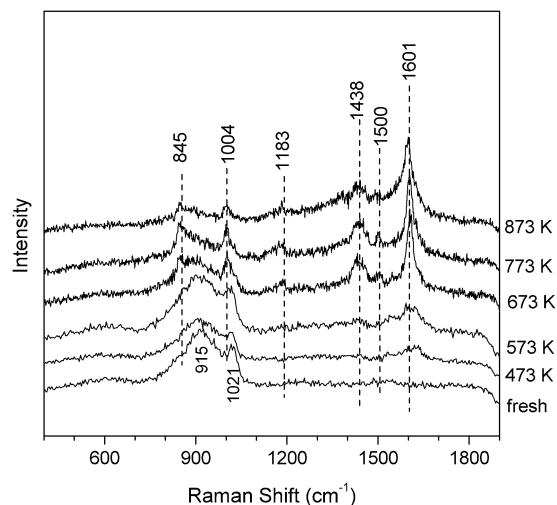


Fig. 4. Raman spectra of butane DH on oxidized 1.2V at different temperatures.

sult is consistent with reduction of the oxidized VO_x sample under butane DH at 873 K.

The Raman spectra collected after butane DH at different temperatures on the oxidized 1.2V sample are shown in Fig. 4. At temperatures below 673 K, a weak Raman band at 1620 cm^{-1} , assigned to C=C stretching in polyolefins, is observed together with the two bands at 1021 and 915 cm^{-1} due to V=O and V–O–Al modes of surface VO_x species, respectively. After butane DH at 673 and 773 K, an intense band at 1601 cm^{-1} due to polyaromatic hydrocarbons develops. Simultaneously, bands at 1500, 1438, 1183, 1004, and 845 cm^{-1} are also observed. Meanwhile, Raman bands at 1021 and 915 cm^{-1} from surface VO_x species are no longer observable, due to a combination of the reduction of VO_x species [5,27–30] and the strong optical absorption by surface coke species. The band at 1500 cm^{-1} is usually assigned to conjugated polyolefins or cyclopentadienyl species [24,33]. The band at 1438 cm^{-1} is due to the bending mode of CH_3/CH_2 or C–H in aromatic rings. C–H bending in aromatics usually appears near 1180 cm^{-1} . The two sharp bands at 1004 and 845 cm^{-1} are rarely reported for coke species in the literature and thus might be ascribed to surface VO_x species. However, the absence of an isotope shift on an ^{18}O -exchanged V/ $\theta\text{-Al}_2\text{O}_3$ sample confirms that these bands are due to surface coke deposits. As the DH temperature is increased to 873 K, the intensity of the Raman bands below 1500 cm^{-1} decreases significantly. Raman spectra obtained after the reaction of butane with pre-reduced 1.2V (not shown) are very similar to those on pre-oxidized 1.2V. This again suggests that the initial valence state of surface VO_x does not affect the nature of coke species, and most likely the VO_x species is partly reduced under butane DH conditions. This conclusion can also be inferred from the similar activity/selectivity results from butane DH tests on either oxidized or pre-reduced 1.2V (not shown here).

Fig. 5 shows the Raman spectra of butane DH on the oxidized 14.2V sample at different temperatures. In addition to the bands at 1026 and 915 cm^{-1} due to dispersed surface VO_x , Raman bands due to crystalline V_2O_5 are also observed at 995, 706, 518, and 483 cm^{-1} . Reduction of surface VO_x species

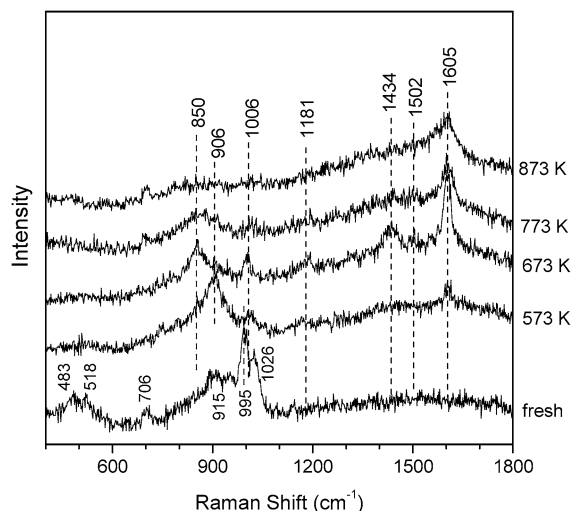


Fig. 5. Raman spectra of butane DH on oxidized 14.2V at different temperatures.

occurs when the sample reacts with butane at 573 K. Raman bands due to V_2O_5 disappear, and the band at 1026 cm^{-1} becomes weaker. A new strong band at 906 cm^{-1} dominates the spectrum. This band is likely due to VO_x species produced by the reduction of V_2O_5 by butane. This is confirmed in the spectra from butane DH on V_2O_5 (see Fig. 7). Weak features due to coke species are also present at 1180, 1434, and 1605 cm^{-1} at this reaction temperature. When the reaction was carried out at 673 K, the spectrum becomes very similar to that from butane DH on the 1.2V sample at this temperature. The set of bands at 850, 1006, 1181, 1434, 1502, and 1605 cm^{-1} is present. Another similarity to the 1.2V sample is the weakening of the bands below 1600 cm^{-1} relative to the band at 1605 cm^{-1} with increasing reaction temperature. At 873 K, only the band at 1605 cm^{-1} persists. Butane DH was also conducted on a pre-reduced 14.2V sample, and again, similar Raman features due to coke species were observed as on oxidized 14.2V.

One important general characteristic of coke is its topology, which can be assessed by the intensity ratio of the band at around 1600 cm^{-1} (G band) to the band at around 1400 cm^{-1} (D band) [24,26]. UV Raman spectra from a series of polyaromatic compounds [24,34] show that the intensity in the spectral range $1600\text{--}1650\text{ cm}^{-1}$ is significantly higher than that in the region $1300\text{--}1450\text{ cm}^{-1}$ for coke species with a two-dimensional, sheet-like topology. In contrast, the intensity is more nearly equal in these two spectral regions for coke species with chainlike topologies. The topology of coke species formed from butane DH on the various $V/\theta\text{-Al}_2O_3$ catalysts at 873 K is compared in Fig. 6. The intensity ratio of I_G to I_D increases as a function of surface VO_x density. It suggests that the coke species are more hydrogen-deficient on $V/\theta\text{-Al}_2O_3$ with high surface VO_x density—namely, more 2D, sheet-like coke species are formed from butane DH on $V/\theta\text{-Al}_2O_3$ with high surface VO_x density ($>1.2\text{ V/nm}^2$).

3.2.3. Butane DH on V_2O_5

Bulk V_2O_5 was also tested for butane DH, and the Raman spectra are shown in Fig. 7. When contacted with butane, the

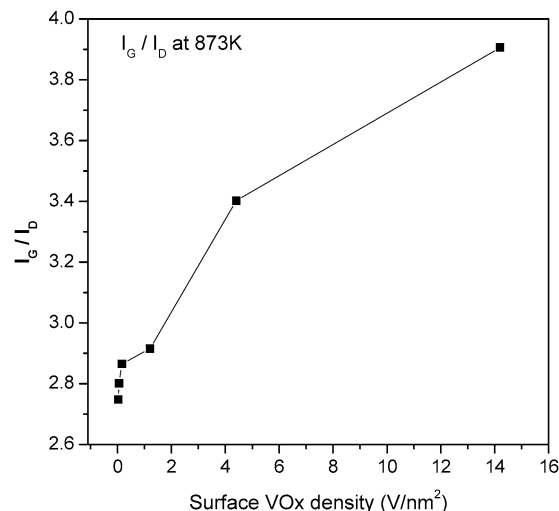


Fig. 6. I_G/I_D measured from the Raman spectra of butane DH at 873 K as a function of surface VO_x density.

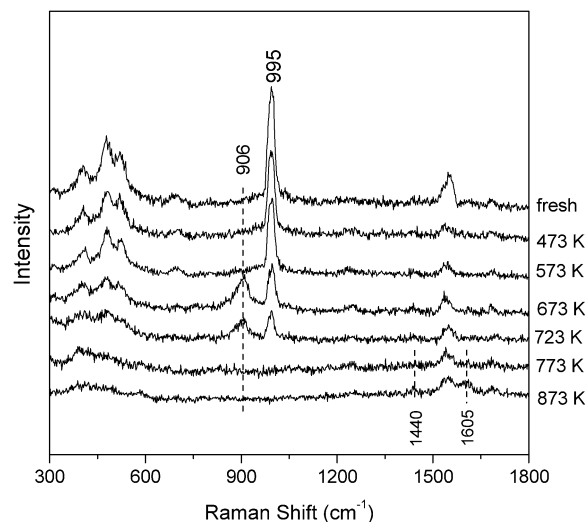


Fig. 7. Raman spectra of butane DH on oxidized V_2O_5 at different temperatures.

Raman bands due to V_2O_5 decrease gradually with increasing temperature and disappear at 873 K, evidence for the reduction of V_2O_5 . A band at 906 cm^{-1} is also observed in the temperature range 673–723 K, possibly due to an intermediate species from reduced V_2O_5 . It is seen that very weak bands at 1400 and 1605 cm^{-1} due to coke species are produced only at a reaction temperature of 873 K. Raman spectra of butane DH on a hydrogen-reduced V_2O_5 sample also show weak Raman features due to coke species. This suggests that V_2O_5 is not the main site making coke in butane DH on $V/\theta\text{-Al}_2O_3$ catalysts. The reduction of crystalline V_2O_5 at lower temperature on 14.2V compared with bulk V_2O_5 is likely due to the smaller crystal size of the well-dispersed V_2O_5 on the support, in agreement with previous TPR results [16].

3.2.4. Pulse experiment of butane DH

Fig. 8 shows the Raman spectra from butane DH on the 1.2V sample at 673 K with controlled doses of butane. It is inter-

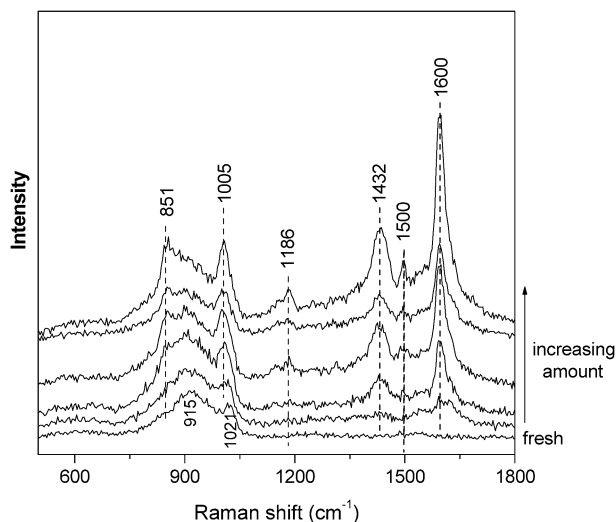


Fig. 8. Raman spectra of butane DH on oxidized 1.2V at 673 K with different dosages of butane.

esting to see that the Raman bands at 851, 1005, 1186, 1432, 1500, and 1600 cm^{-1} appear and grow simultaneously with increasing doses of butane while the bands at 915 and 1021 cm^{-1} due to surface VO_x species vanish gradually. It appears that these bands are from a single surface coke species. Because C_4 olefins (1-butene, 2-butenes, and 1,3-butadiene) are detected from butane DH on $\text{V}/\theta\text{-Al}_2\text{O}_3$ catalysts in the reactivity tests, a Raman study of their reactions with the supported VO_x catalysts can be expected not only to help assign the set of Raman bands, but also to provide information on which of these olefins are the coke precursors.

3.3. Raman Study of $\text{C}_4=$ DH

The reaction of different C_4 olefins was investigated on the 1.2V sample. Fig. 9 presents the Raman spectra from 1-butene, *cis/trans*-2-butenes, and 1,3-butadiene DH on the 1.2V sample. As shown in Fig. 9A, a band at around 1640 cm^{-1} is present at room temperature and up to 573 K, due to olefinic species on the surface. This band is gradually replaced by a strong band at 1603 cm^{-1} as the reaction temperature rises above 573 K. Meanwhile, bands at 851, 1003, 1173, 1385, 1440, and 1502 cm^{-1} also grow. Raman bands due to surface VO_x species are not observable at reaction temperatures above 573 K. These spectral features from 1-butene DH are very similar to those observed from butane DH on the 1.2V sample, suggesting that similar coke species are formed from both 1-butene reaction and butane DH with increasing reaction temperature. Raman spectra from *cis*-2-butene and *trans*-2-butene DH on the 1.2V sample are identical, and thus Fig. 9B represents spectra from either of these spectra. These spectra are also very similar to those from 1-butene reaction and butane DH, indicating that the coke species made from 1-butene, *cis*-2-butene, and *trans*-2-butene are similar to those from butane on the 1.2V sample. This result suggests that a common coke precursor is shared between the DH of butane and the C_4 olefins on supported VO_x catalysts. The band near 1640 cm^{-1} , formed on adsorption of

1-butene and 2-butenes at low temperature, may be from surface butadiene species because this band is also observed in both gaseous and adsorbed 1,3-butadiene (Fig. 9C).

Raman spectra after 1,3-butadiene reaction on the 1.2V sample (Fig. 9C) also consist of the set of Raman bands at 850, 1006, 1181, 1446, 1502, and 1605 cm^{-1} for reaction temperatures above 573 K. Thus, 1,3-butadiene also contributes to the coke formation in the butane DH reaction on $\text{V}/\theta\text{-Al}_2\text{O}_3$ catalysts. There are some differences in the temperature behavior, however. For example, these bands are already present on room temperature adsorption of 1,3-butadiene on the 1.2V sample. The spectrum of gas-phase 1,3-butadiene is included for comparison. Apparently, 1,3-butadiene reacts on adsorption on the catalyst surface. Considering the low temperature (298 K), a possible chemical change for 1,3-butadiene is its cyclization to form styrene on the surface. Comparing the spectrum (Fig. 9D-a) from styrene to that after butane DH at 673 K on 1.2V (Fig. 9D-b) reveals a very similar set of bands. Also included is the spectrum from a mixture of 1.2V with styrene heated at 393 K (Fig. 9D-c). Styrene is known to polymerize easily on heating. Comparison of spectrum c to that reported for polystyrene [35] confirms the identity of spectrum c; the set of Raman bands near 850, 1002, 1183, 1437, 1501, and 1603 cm^{-1} is due to polystyrene. Thus, it appears that polystyrene is a key intermediate in the coke formation process during butane DH on the 1.2V catalyst.

Reaction of 1,3-butadiene on the other $\text{V}/\theta\text{-Al}_2\text{O}_3$ samples was also conducted; the Raman spectra show the presence of the polystyrene bands at reaction temperatures above 573 K, suggesting that both monovanadates and polyvanadates make polystyrene from butane DH at high temperatures. A key difference is that these bands are much weaker than those due to either $\theta\text{-Al}_2\text{O}_3$ or surface VO_x species on samples with lower VO_x density than on those with higher VO_x density, reflecting the difference in the amount of polystyrene on the surface.

3.4. Oxidation of coke species

Regeneration of the coked $\text{V}/\theta\text{-Al}_2\text{O}_3$ catalysts was attempted by oxidation. This was done both in the fluidized-bed reactor with monitoring by Raman spectroscopy and in the U-shaped reactor with on-line gas chromatography. Fig. 10 gives the Raman spectra of the coked 1.2V sample (after butane DH at 873 K) reoxidized at different temperatures. The bands due to coke species disappear completely after oxidation above 773 K. Meanwhile, Raman bands due to surface VO_x species appear to be completely restored at 873 K, indicating that the catalyst structure is regenerated after coke removal. The reoxidation of other coked $\text{V}/\theta\text{-Al}_2\text{O}_3$ catalysts shows similar Raman features, except that the coke removal temperature depends on the surface VO_x density: the higher the surface VO_x density, the lower the removal temperature. This is confirmed by the TPO results (Fig. 11A). The main TPO peak shifts from ca. 750 K on the 0.06V sample to 660 K on the 14.2V and V_2O_5 samples. The amount of coke in monolayers quantified from the TPO profiles is plotted in Fig. 11B as a function of surface VO_x density. The

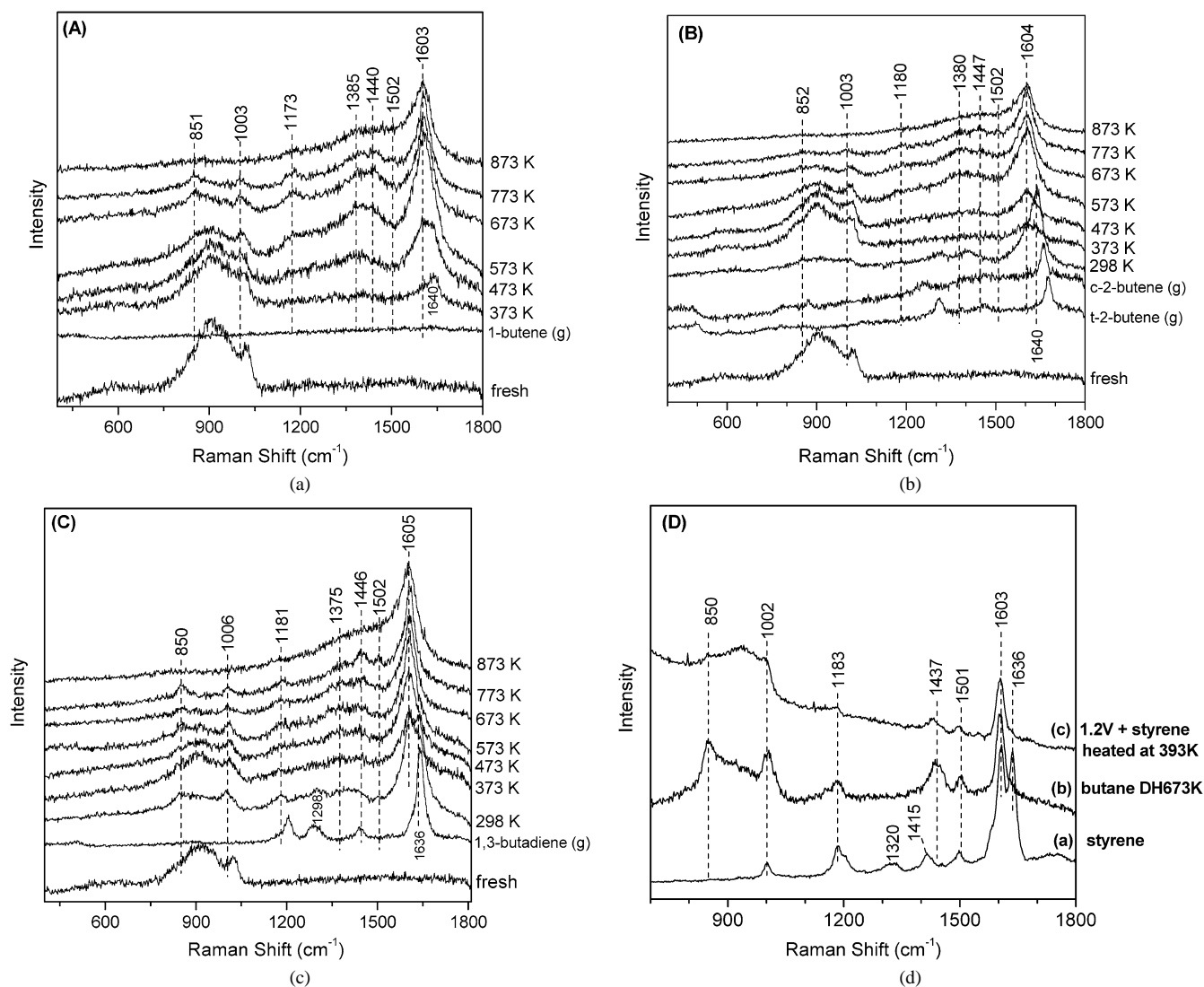


Fig. 9. Raman spectra of 1-butene (A), *cis/trans*-2-butenes (B), 1,3-butadiene (C) DH on oxidized 1.2V at different temperatures. (D) Comparison of Raman spectra from styrene (a), butane DH on 1.2V at 673 K (b), and a mixture of 1.2V and styrene 1.2V at 393 K (c).

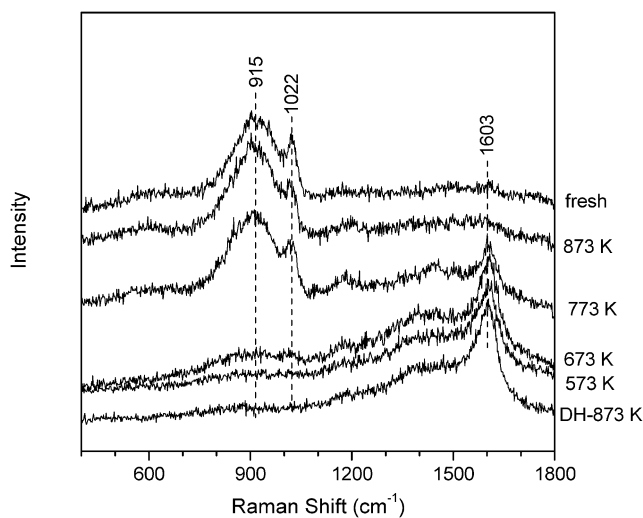


Fig. 10. Raman spectra of coked 1.2V reoxidized at different temperatures.

amount of coke increases with VO_x loading on the surface of Al₂O₃.

4. Discussion

4.1. Structure–coke relationship

The existing studies of supported VO_x catalysts for light alkane DH focused on either the pretreatment or support effects on the DH activity and selectivity [11–15]. Coke formation chemistry has rarely been investigated on supported VO_x [28] catalysts. The results presented here provide insight into the structure–coke formation relationship in the DH of butane on V/ θ -Al₂O₃ catalysts.

The amount and nature of the coke species formed in butane DH depends on the structure of the surface VO_x species. Olefin/polyolefin species are the only coke deposits on the θ -Al₂O₃ surface at reaction temperature up to 873 K. They are also the main coke species made by V/ θ -Al₂O₃ catalysts

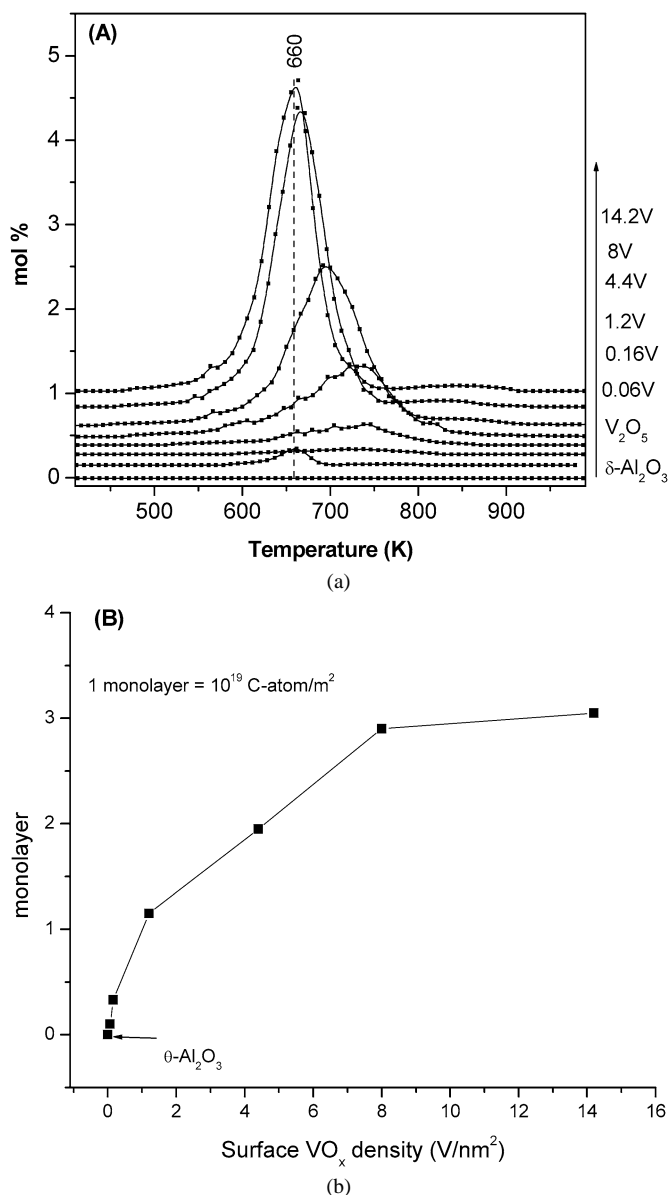


Fig. 11. (A) TPO profiles (CO₂ + CO) of θ -Al₂O₃, V₂O₅, and V/ θ -Al₂O₃ coked in butane at 873 K for 90 min. (B) Amount of coke (1 monolayer $\sim 10^{19}$ C atom/m²) as a function of surface VO_x density.

with only monovanadate species at reaction temperatures below 873 K. On all V/ θ -Al₂O₃ catalysts, polyaromatics are produced on the surface at 873 K, which is the normal operation temperature for DH reactions. But the topology of the polyaromatics on V/ θ -Al₂O₃ catalysts varies depending on the surface VO_x species (see Fig. 6). The results indicate that the polyaromatics become more 2D sheetlike on V/ θ -Al₂O₃ as the surface VO_x density increases. Our recent study [16,36] showed that a mixture of monovanadate and polyvanadates is present on V/ θ -Al₂O₃ samples with surface VO_x densities >0.16 V/nm². The polyvanadate species increase in amount (and possibly also in cluster size) as the VO_x loading increases and eventually produce crystalline V₂O₅. Thus, it appears that 2D polyaromatics are likely formed on polyvanadates, whereas 1D, chainlike polyaromatics are produced exclusively by monovanadates in

the DH of butane at 873 K. The 2D polyaromatics presumably can reorganize into pregraphitic entities that have been demonstrated to be the kind of coke that causes the deactivation of DH catalysts [32,37,38]. Polyaromatic species can also be made by crystalline V₂O₅ (Fig. 7).

Within this picture, the activity behavior of the V/ θ -Al₂O₃ catalysts in butane DH (Fig. 1A) can be explained. The decline of initial activity for the 14.2V sample is likely due to the formation of V₂O₅ on the surface, because crystalline V₂O₅ typically has very small surface area. Therefore, the dispersed VO_x species are much more active than crystalline V₂O₅. However, the initially high activity of catalysts with high VO_x density (i.e., more polyvanadates) is achieved at the price of fast deactivation. The remarkable decline of butane DH activity for V/ θ -Al₂O₃ catalysts with high surface VO_x density (>1.2 V/nm²) can be attributed to the formation of detrimental 2D polyaromatics on polyvanadates, which are the major VO_x species on the surface. The stable reactivity performance of the V/ θ -Al₂O₃ catalysts with surface VO_x density <1.2 V/nm² is due to the restricted formation of only chainlike polyaromatics on monovanadate. For the 1.2 V sample, our analysis [36] shows that about half of the surface VO_x is monovanadate and the other half is polyvanadate. The stable activity of the 1.2V sample may be the result of polyvanadate clusters that are still small in size and diluted by adjacent monovanadate species. This picture is similar to the sulfur passivation effect on PtRe/Al₂O₃ catalysts [39,40] where rhenium poisoned by sulfur is considered inert and serves to divide the platinum surface into smaller ensembles. The transformation of hydrocarbonaceous fragments into pseudographite is impeded in the conversion of *n*-hexane over these catalysts, and the PtRe/Al₂O₃ catalyst remains stable. In analogy, we suggest that the dilution effect of monovanadate prevents the formation of 2D polyaromatics on polyvanadates, so that the 1.2V catalyst maintains stable activity under butane DH conditions. As the amount of monovanadate decreases with surface VO_x density, and the polyvanadate clusters increase in size and frequency on the support, the catalyst is more prone to form 2D coke species that eventually lead to the deactivation of V/ θ -Al₂O₃ catalysts. Therefore, it appears that an optimal V/ θ -Al₂O₃ catalyst for butane DH should have both size- and proximity-controlled VO_x clusters with density as high as possible. Such a catalyst can be both highly active and stable.

Although the V/ θ -Al₂O₃ catalysts show deactivation to some extent in butane DH, the selectivity to C₄ olefins (1-butene, 2-butenes, and 1,3-butadiene) increases with reaction time (see Fig. 1B). Because the C₄ olefins selectivity shows a similar trend on both oxidized and prerduced V/ θ -Al₂O₃ catalysts in butane DH, the selectivity change cannot be due to the reduction of surface VO_x. Rather, it appears that coke deposits on the surface are beneficial for olefin selectivity, an idea that has also been suggested in previous studies of hydrocarbon conversions [12,41,42]. Because Lewis acid sites present on θ -Al₂O₃ tend to catalyze the cracking of butane [15], the blocking of acid sites by coke species could be responsible for the increased selectivity to C₄ olefins with time on steam on V/ θ -Al₂O₃ catalysts with low surface VO_x densities. For the samples with high surface VO_x densities, the increase in se-

lectivity to C_4 olefins with reaction time is likely due to the deactivation of surface active sites responsible for total oxidation. This suggestion is supported by the observation that an initially high selectivity to CO_x (ca. 30%) decreases simultaneously with increasing $C_{4=}$ selectivity on $V/\theta-Al_2O_3$ catalysts with high VO_x densities.

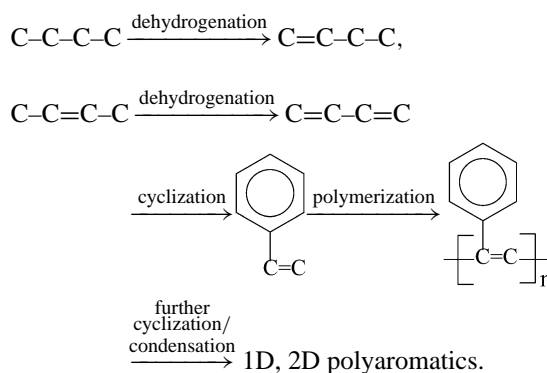
The amount of coke formed in butane DH is also related to the structure of VO_x species, as demonstrated in the quantification of the TPO results (Fig. 11). Obviously, the coke amount follows this sequence: polyvanadates > monovanadate > V_2O_5 , $\theta-Al_2O_3$. The amounts of coke deposited on the catalyst surfaces are high enough to cause active site poisoning as well as pore blocking. After 90 min on stream, the coverage of carbon on the catalyst surface ranges from ca. 0.1 monolayer on 0.06V to 3 monolayer on the 14.2V sample. Consequently, it is reasonable to attribute the deactivation of $V/\theta-Al_2O_3$ catalysts in butane DH to coke formation.

Structural information about VO_x species under butane DH conditions is also obtainable from the results presented here. The decrease in intensity of the Raman bands due to surface VO_x species on the 0.03V sample in butane DH at 873 K (Fig. 3) indicates the reduction of VO_x species, consistent with other Raman studies on alkane dehydrogenation over supported vanadia catalysts [5,27,28,30]. When V_2O_5 is present in the sample (i.e., for 14.2V and bulk V_2O_5), the reduction is more obvious, as evidenced by the disappearance of the 995-cm^{-1} band and the appearance of a new band at 906-cm^{-1} even at low temperature. The intense band at 906-cm^{-1} , which has not been reported in previous Raman studies of supported vanadia samples under alkane DH [5,27,28,30], is probably due to an intermediate state in the reduction of bulk vanadia, because it disappears at higher reaction temperatures (above 773 K). The Raman spectra of bulk vanadium oxides, including V_2O_5 , V_6O_{13} , VO_2 , and V_2O_3 , were measured in our lab, and none gave a band at ca. 906-cm^{-1} . Although the vanadia phase associated with this band has not been identified, its presence is an indication that vanadia species undergo reduction during butane dehydrogenation. Although the Raman bands due to surface VO_x species are not observable at 873 K due to the presence of coke species on $V/\theta-Al_2O_3$ catalysts with higher VO_x density, the similarity of coke species formed on both preoxidized and prerduced samples (i.e., their similar coke formation chemistry) suggests that the surface VO_x species are in a reduced state under butane DH conditions. The reduction of surface VO_x species is also inferred from the activity tests. During the initial stage of butane DH, a certain amount of CO_x is detected. Once this initial period is completed, no significant amount of CO_x is detected, with most of the observed products being hydrocarbon species. Thus, one could envisage that the oxidized VO_x species undergo a reduction process during the initial stage of butane DH. The structure of the VO_x species can be regenerated after the oxidative removal of coke deposits (see Fig. 10), and the coke removal temperature is a function of the VO_x density. It appears that a large portion of the coke is located on the support for $V/\theta-Al_2O_3$ catalysts with low VO_x density and thus is difficult to oxidize, whereas more coke deposits onto VO_x clusters as the VO_x density increases. The latter coke species

can be easily oxidized because VO_x clusters are obviously better than Al_2O_3 in oxidation reactions. The change in location of coke species on $V/\theta-Al_2O_3$ catalysts with different VO_x density is consistent with the selectivity increase observed in the reactivity tests (Fig. 1B).

4.2. Coke formation process in butane DH

Insights into the coke formation process in butane DH on $V/\theta-Al_2O_3$ catalysts are made possible in this work by Raman studies of the reactions of butane, 1-butene, *cis/trans*-2-butenes, and 1,3-butadiene at different temperatures. Comparison of the Raman spectra (Fig. 9) from 1-butene, 2-butenes, and 1,3-butadiene reactions with those from butane DH suggests that these C_4 olefins are possible coke precursors in butane DH. The similarity of the Raman spectra between 1-butene, 2-butenes, and 1,3-butadiene at room temperature implies that the adsorption of 1-butene and 2-butenes onto $V/\theta-Al_2O_3$ catalysts produces adsorbed 1,3-butadiene species. Adsorbed 1,3-butadiene species can be easily cyclized into styrene at low temperature and then polymerized to form polystyrene at elevated reaction temperature. To our knowledge, this is the first report indicating that polystyrene is a key intermediate in the coke formation process in butane DH. As the DH temperature is further increased to 873 K, polystyrene species develop further into 1D or 2D polyaromatics, depending on the structure of surface VO_x species. Based on these observations, a coke formation pathway in butane DH on $V/\theta-Al_2O_3$ can be proposed as follows:



5. Conclusions

A structure–coke relationship was established in the DH of butane on $V/\theta-Al_2O_3$ catalysts by reactivity and UV Raman investigations. Both the nature and amount of coke show a dependence on the structure of the $V/\theta-Al_2O_3$ catalysts. Polyaromatics are the main coke species formed under butane DH conditions at 873 K, but the coke species are 2D-like on polymeric VO_x and chainlike on monomeric VO_x . $V/\theta-Al_2O_3$ catalysts with more polyvanadates deactivate faster than those with more monovanadates in butane DH, because of the preferable formation of more 2D-like coke deposits. The amount of coke formed in butane DH follows this sequence: polymeric VO_x > monomeric VO_x > V_2O_5 , Al_2O_3 .

The coke species from butane DH on $V/\theta-Al_2O_3$ catalysts are proposed to form with polystyrene as a key intermediate

and 1-butene, 2-butenes, and 1,3-butadiene as the precursors. Surface VO_x species are in a reduced state under butane DH conditions. The structure of VO_x species can be fully resumed by oxidation of the coke deposits up to 873 K.

Acknowledgments

This work was supported by ATHENA and the Chemical Sciences, Geosciences and Biosciences Division, Office of Basic Energy Sciences, Office of Science, US Department of Energy (grant DE-FG02-97ER14789). The Athena project is funded by the Engineering & Physical Sciences Research Council (EPSRC) of the UK and Johnson Matthey plc.

References

- [1] S. Albonetti, F. Cavani, F. Trifiro, *Catal. Rev.* (1996) 413.
- [2] J.M. McNamara, S.D. Jackson, D. Lennon, 81 (2003) 583.
- [3] E.A. Mamedov, V.C. Corberan, *Appl. Catal. A: Gen.* 127 (1995) 1.
- [4] T. Blasco, J.M.L. Nieto, *Appl. Catal. A: Gen.* 157 (1997) 117.
- [5] F. Cavani, F. Trifiro, *Catal. Today* 24 (1995) 307.
- [6] I.E. Wachs, J. Jehng, G. Deo, B.M. Weckhuysen, V.V. Gulians, J.B. Benziger, S. Sundaresan, *J. Catal.* 170 (1997) 75.
- [7] L.M. Madeira, M.F. Portela, *Catal. Rev.* 44 (2002) 247.
- [8] M.D. Argyle, K. Chen, A.T. Bell, E. Iglesia, *J. Catal.* 208 (2002) 139.
- [9] N. Mimura, M. Saito, *Catal. Today* 55 (2000) 173.
- [10] C.-Y. Shiau, S. Chen, J.C. Tsai, S.I. Lin, *Appl. Catal. A: Gen.* 198 (2000) 95.
- [11] M.A. Chaar, D. Patel, H.H. Kung, *J. Catal.* 109 (1988) 463.
- [12] M.E. Harlin, V.M. Niemi, A.O.I. Krause, *J. Catal.* 195 (2000) 67.
- [13] M.E. Harlin, V.M. Niemi, A.O.I. Krause, B.M. Weckhuysen, *J. Catal.* 203 (2001) 242.
- [14] S.D. Jackson, D. Lennon, G. Webb, J. Willis, *Stud. Surf. Sci. Catal.* 139 (2001) 271.
- [15] M. Volpe, G. Tonetto, H. de Lasa, *Appl. Catal. A: Gen.* 272 (2004) 69.
- [16] Z. Wu, H.S. Kim, S. Rugmini, S.D. Jackson, P.C. Stair, *J. Phys. Chem. B* 109 (2005) 2793.
- [17] C. Li, P.C. Stair, *Stud. Surf. Sci. Catal.* 101 (1996) 881.
- [18] C. Li, P.C. Stair, *Catal. Today* 33 (1997) 353.
- [19] Y.T. Chua, P.C. Stair, *J. Catal.* 196 (2000) 66.
- [20] S. Xie, E. Iglesia, A.T. Bell, *Langmuir* 16 (2000) 7162.
- [21] M. Bowker, T. Aslama, M. Roebuck, M. Moser, *Appl. Catal. A: Gen.* 257 (2004) 57.
- [22] S. Carra, L. Forni, *Catal. Rev.* 5 (1971) 159.
- [23] M.J. Ledoux, F. Meunier, B. Heinrich, C. Pham-Huu, M.E. Harlin, A.O.I. Krause, *Appl. Catal. A: Gen.* 181 (1999) 157.
- [24] Y.T. Chua, P.C. Stair, *J. Catal.* 213 (2003) 39.
- [25] J. Li, G. Xiong, Z. Feng, Z. Liu, Q. Xin, C. Li, *Microporous Mesoporous Mater.* 39 (2000) 275.
- [26] S. Kuba, H. Knozinger, *J. Raman Spectrosc.* 33 (2002) 39.
- [27] M.A. Banares, I.E. Wachs, *J. Raman Spectrosc.* 33 (2002) 359.
- [28] G. Mul, M.A. Banares, G. Garcia Cortez, B. van der Linden, S.J. Khatib, J.A. Moulijn, *Phys. Chem. Chem. Phys.* 5 (2003) 4378.
- [29] J.M. Kanervo, M.E. Harlin, A.O.I. Krause, M.A. Banares, *Catal. Today* 78 (2003) 171.
- [30] A. Christodoulakis, M. Machli, A.A. Lemonidou, S. Boghosian, *J. Catal.* 222 (2004) 293.
- [31] D. Espinat, H. Dexpert, E. Freund, G. Marino, M. Couzi, P. Lespade, F. Cruege, *Appl. Catal.* 16 (1985) 343.
- [32] S.M.K. Airaksinen, M.A. Banares, A.O.I. Krause, *J. Catal.* 230 (2005) 507.
- [33] A. Baruya, D.L. Gerrard, W.F. Maddams, *Macromolecules* 16 (1983) 578.
- [34] S.A. Asher, *Anal. Chem.* A 65 (1993) 201.
- [35] L.K. Noda, O. Sala, *Spectrochim. Acta A* 56 (1999) 145.
- [36] Z. Wu, P.C. Stair, manuscript in preparation.
- [37] S.M. Davis, F. Zaera, G.A. Somorjai, *J. Catal.* 77 (1982) 439.
- [38] S.J. Tinnemans, M.H.F. Kox, T.A. Nijhuis, T. Visser, B.M. Weckhuysen, *Phys. Chem. Chem. Phys.* 7 (2005) 211.
- [39] W.M.H. Sachtler, *J. Mol. Catal.* 25 (1984) 1.
- [40] V.K. Shum, J.B. Butt, W.M.H. Sachtler, *J. Catal.* 96 (1985) 371.
- [41] J.R. Rostrup-Nielsen, *Stud. Surf. Sci. Catal.* 68 (1991) 85.
- [42] A. Hakuli, A. Kytokivi, A.O. Krause, T. Suntola, *J. Catal.* 161 (1996) 393.